

Supplementary Information

Crystallization of CsPbBr₃ single crystals in water for X-ray detection

Jiali Peng,¹ Chelsea Q. Xia,² Yalun Xu,¹ Ruiming Li,¹ Lihao Cui,¹ Jack K. Clegg,³
Laura M. Herz,² Michael B. Johnston,² and Qianqian Lin^{*1}

¹ *Key Lab of Artificial Micro- and Nano-Structures of Ministry of Education of China, School of Physics and Technology, Wuhan University, Wuhan 430072, P. R. China*

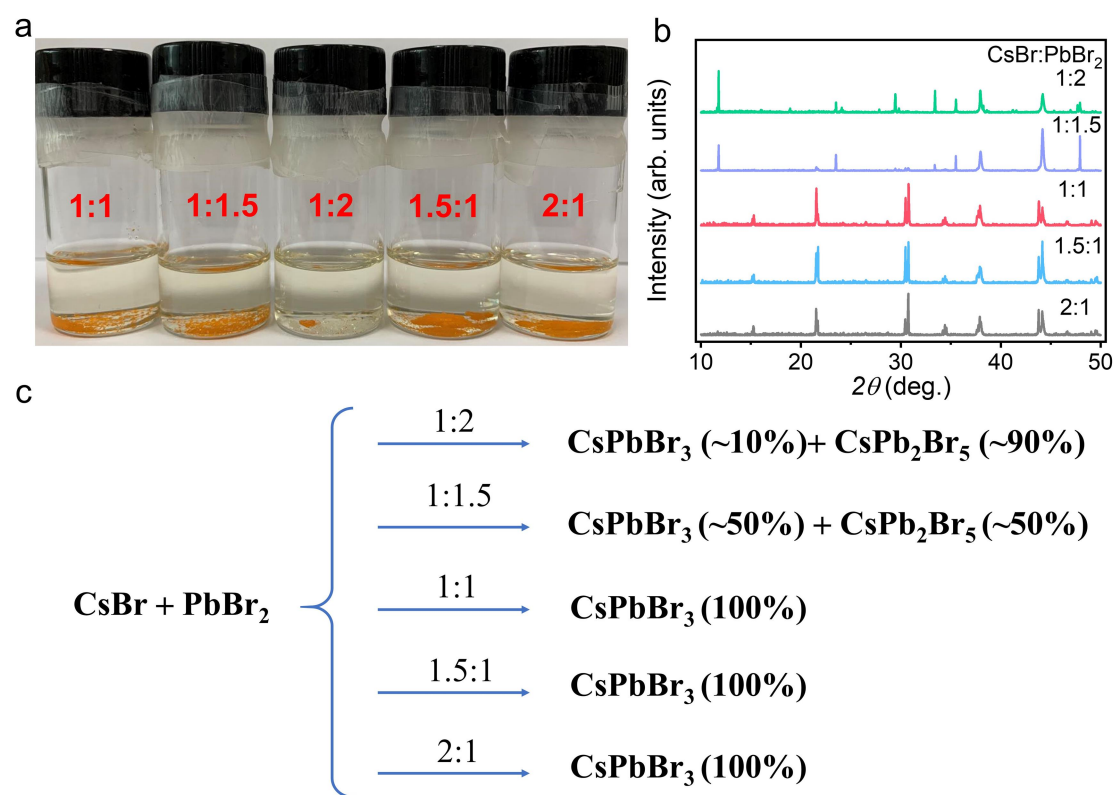
² *Department of Physics, University of Oxford, Clarendon Laboratory, Parks Road, Oxford, OX1 3PU, U.K.*

³ *School of Chemistry and Molecular Biosciences, The University of Queensland, Brisbane, QLD4072, Australia*

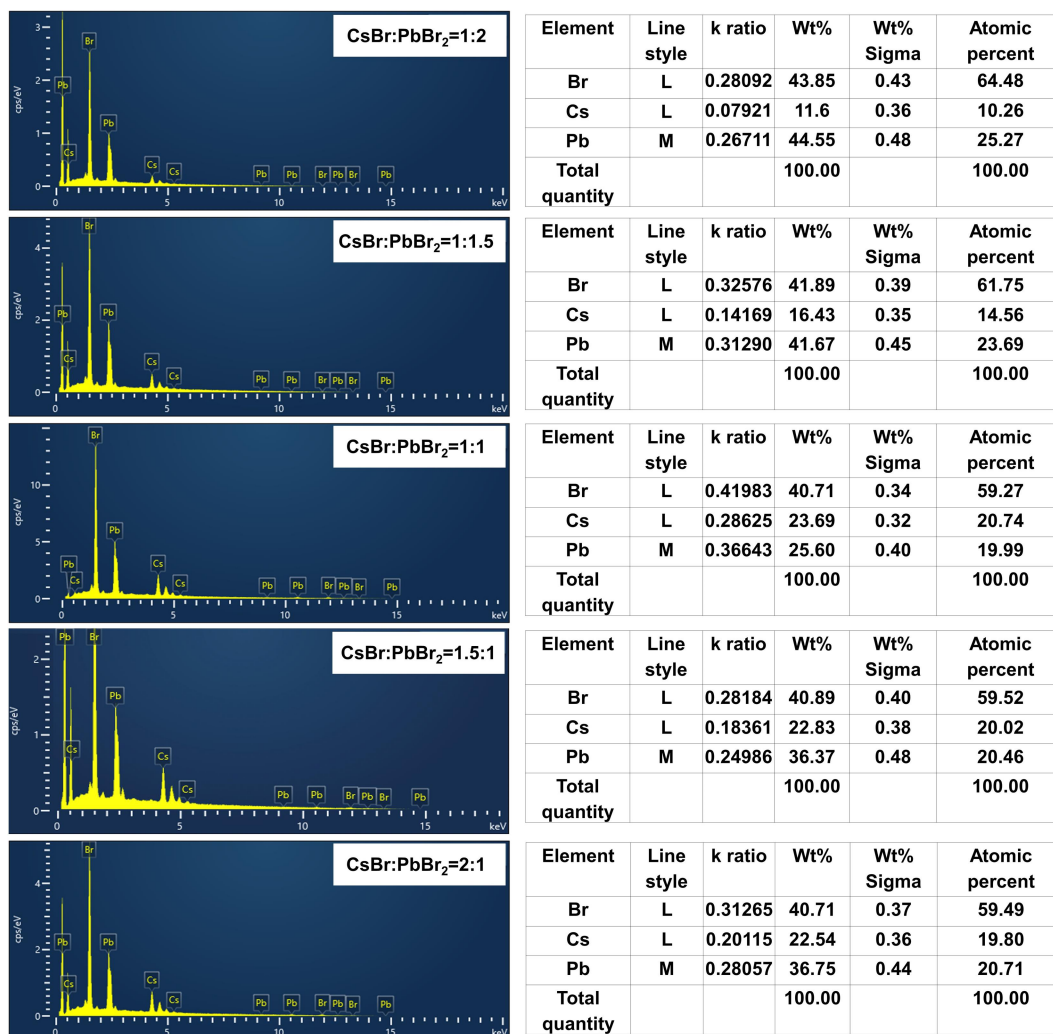
Corresponding Author:

*Email: q.lin@whu.edu.cn

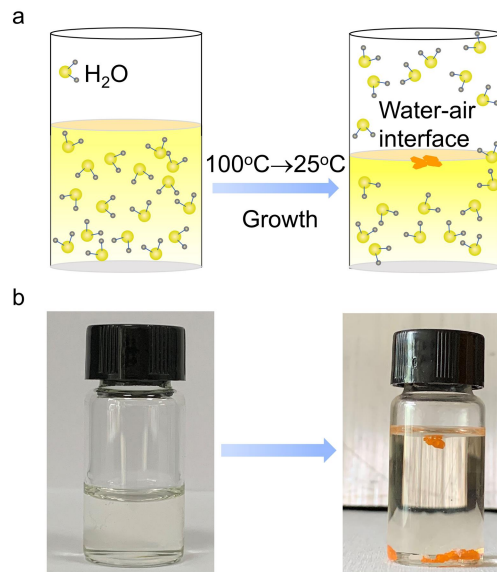
Supplementary Figures



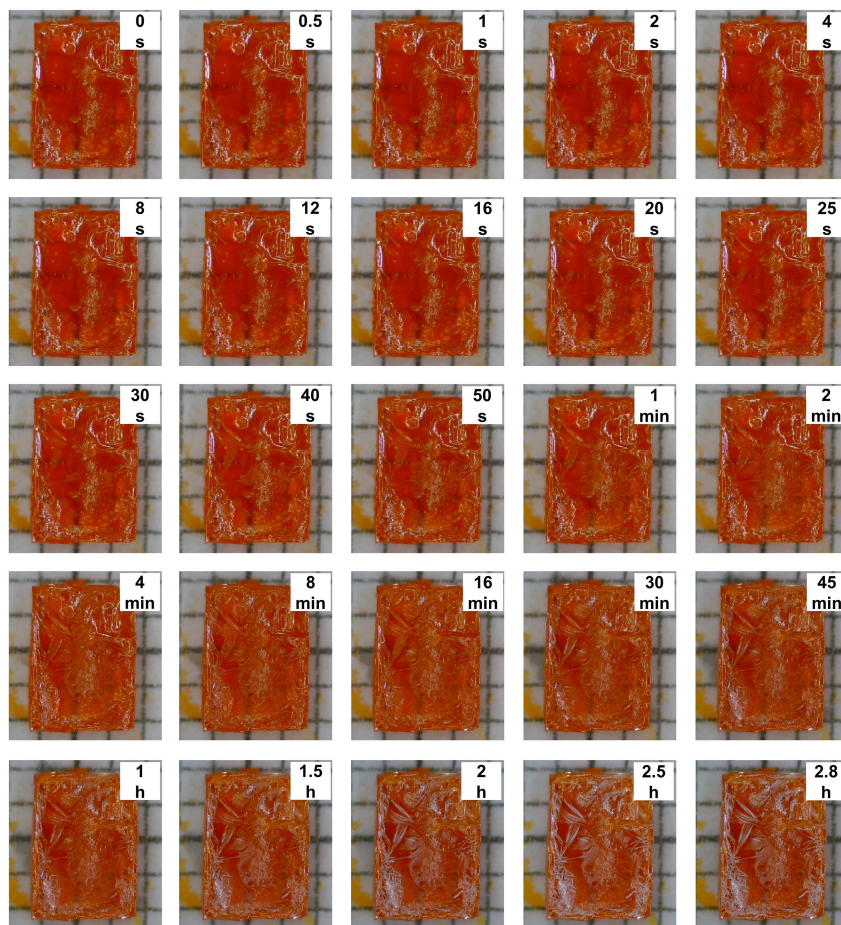
Supplementary Figure 1. (a) Optical photos and (b) powder X-ray diffraction patterns of CsPbBr₃ SCs grown in water with various CsBr:PbBr₂ ratios. (c) Schematic illustration of the crystallization routes with different precursor composition.



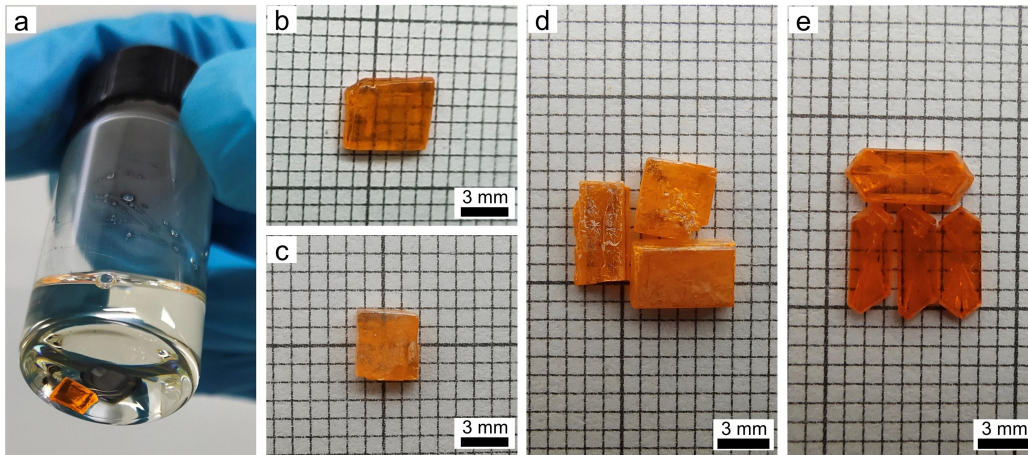
Supplementary Figure 2. Energy dispersive spectroscopy (EDS) analysis of CsPbBr₃ SCs grown with different CsBr:PbBr₂ ratios in precursor solution.



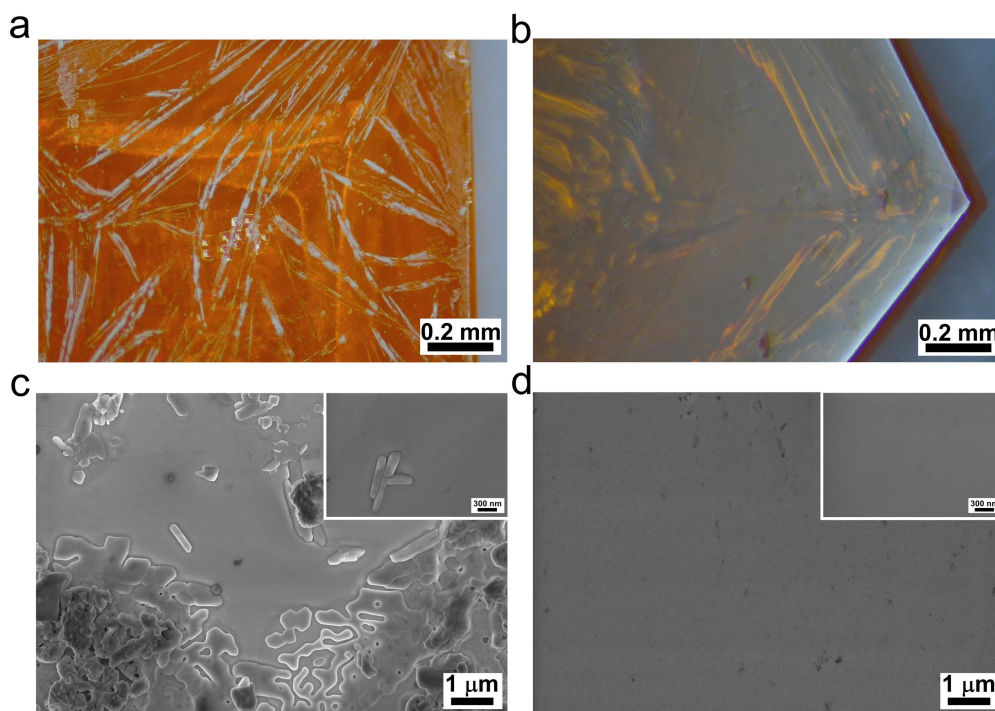
Supplementary Figure 3. (a) Schematic illustration and (b) optical photos of the formation of CsPbBr₃ SCs at the water/air interface.



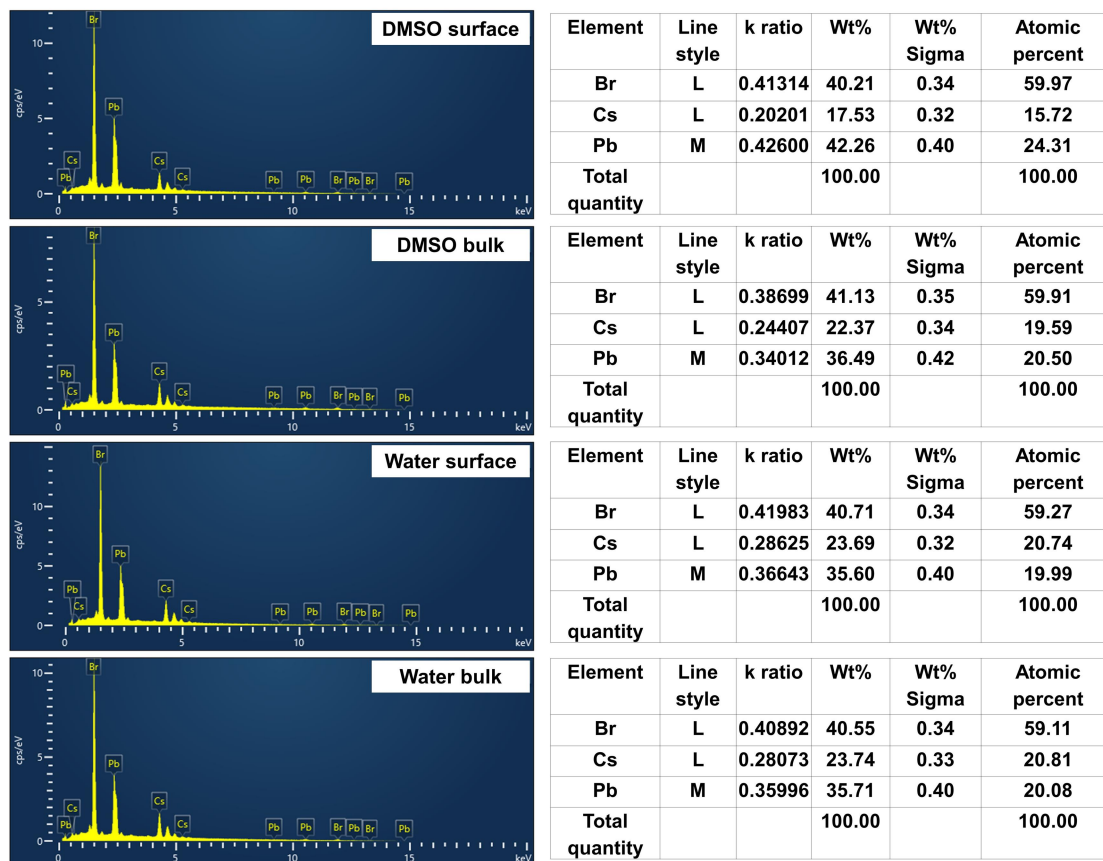
Supplementary Figure 4. Surface morphology evolution of the CsPbBr₃ SCs grown in DMSO, recorded with optical microscope.



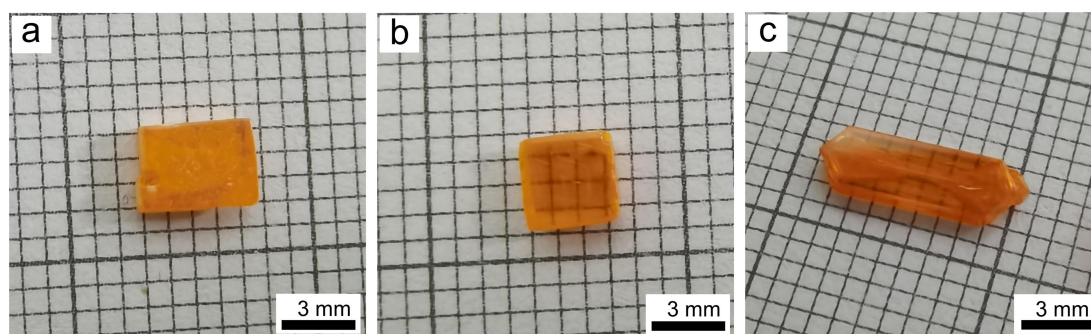
Supplementary Figure 5. Optical photo of (a) DMSO-grown CsPbBr₃ SCs in DMSO, comparison of DMSO-grown CsPbBr₃ SCs prepared and dried (b) in glovebox and (c) in air, comparison of the long-term air stability of the CsPbBr₃ SCs grown (d) in DMSO and (e) in water after exposed in air for one week.



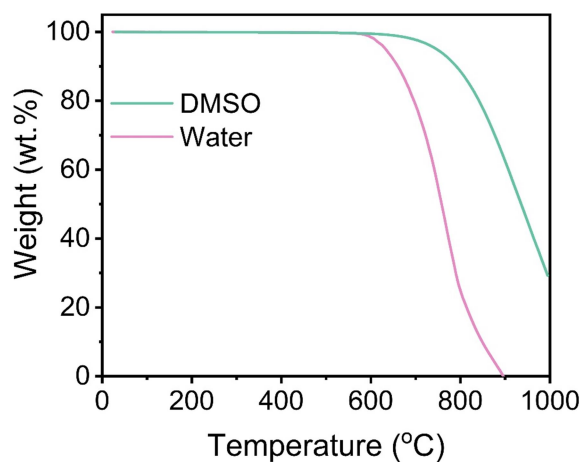
Supplementary Figure 6. Typical optical photos of CsPbBr₃ SCs grown in (a) DMSO and (b) water after exposure in air (40% RH) for 3 hours, SEM images the surface morphology of CsPbBr₃ SCs grown in of (c) DMSO and (b) water after exposure in air (40% RH) for 3 hours.



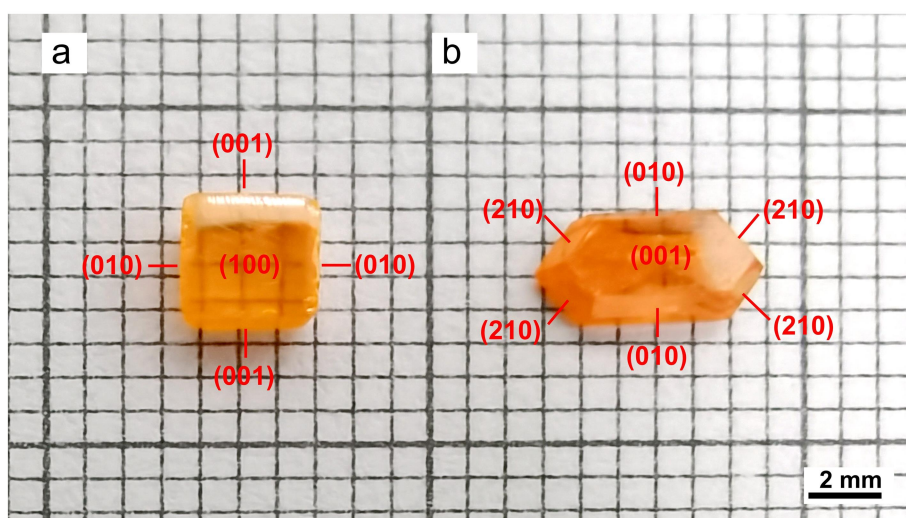
Supplementary Figure 7. Energy dispersive spectroscopy (EDS) analysis of the surface and bulk composition of CsPbBr₃ SCs grown in DMSO and water.



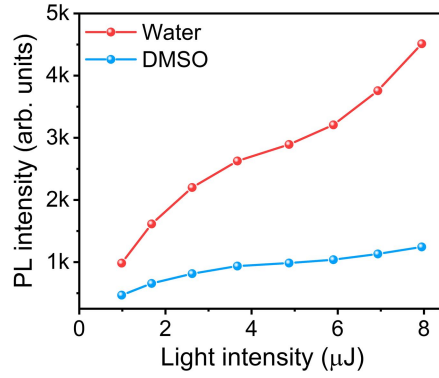
Supplementary Figure 8. Comparison of the optical photos of (a) as-prepared DMSO-grown, (b) polished DMSO-grown and (c) as-prepared water-grown single crystals. The polished DMSO-grown single crystals exhibited very reflective and smooth surface, and have similar transparency as the water-grown crystals.



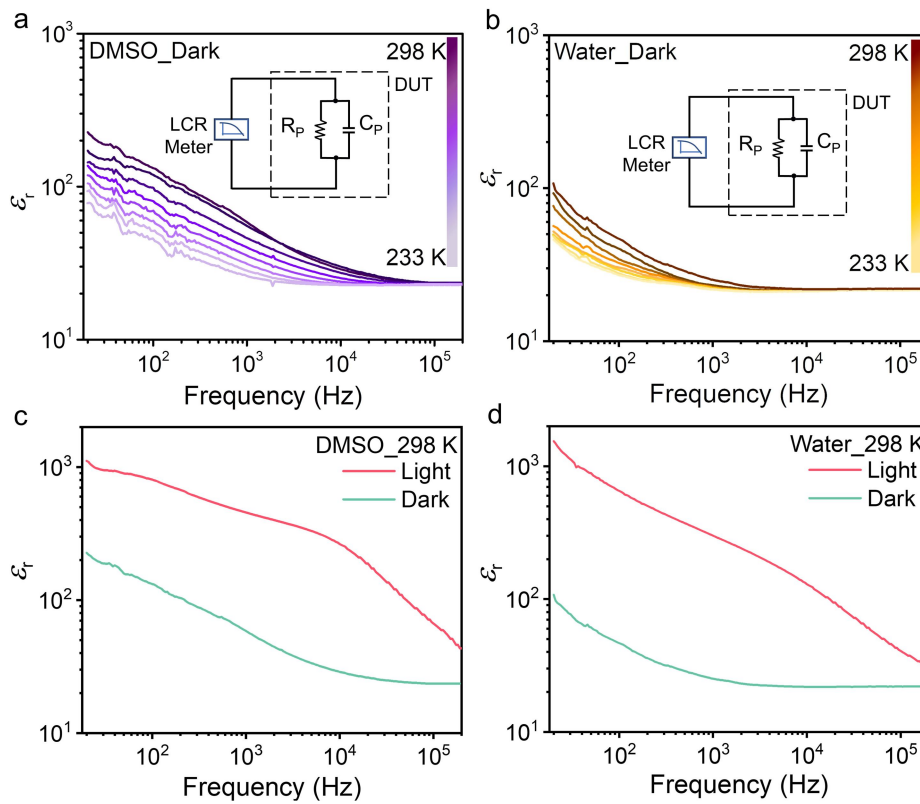
Supplementary Figure 9. Comparison of the thermal gravimetric analysis (TGA) of CsPbBr₃ SCs grown in DMSO and water.



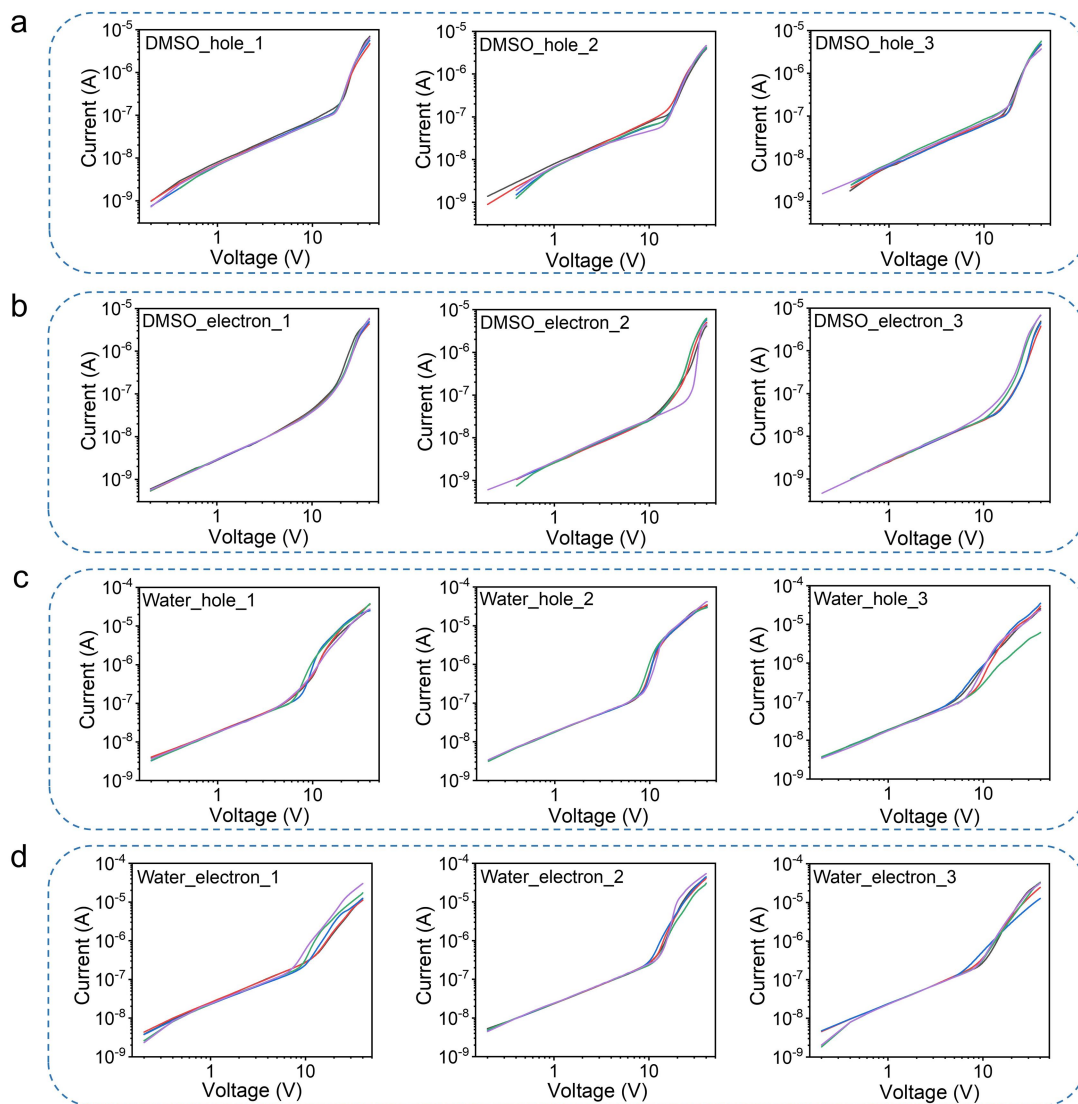
Supplementary Figure 10. Typical optical photos with face-indexing of CsPbBr₃ SCs grown in (a) DMSO and (b) water.



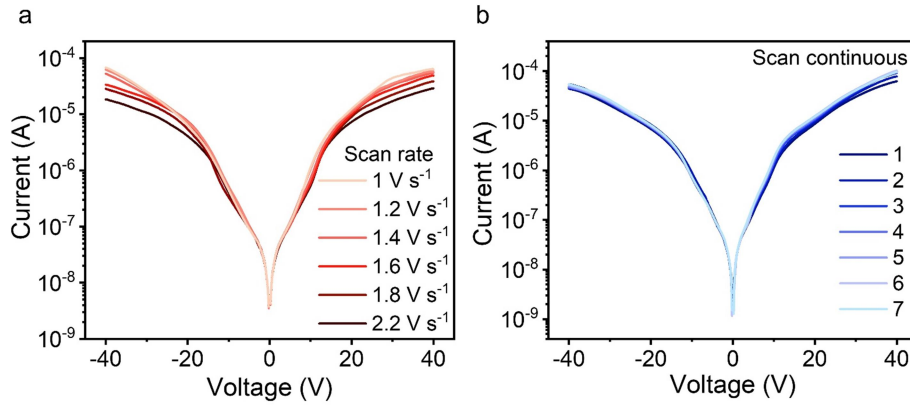
Supplementary Figure 11. Fluence-dependent PL intensity of the DMSO and water-grown CsPbBr₃ SCs.



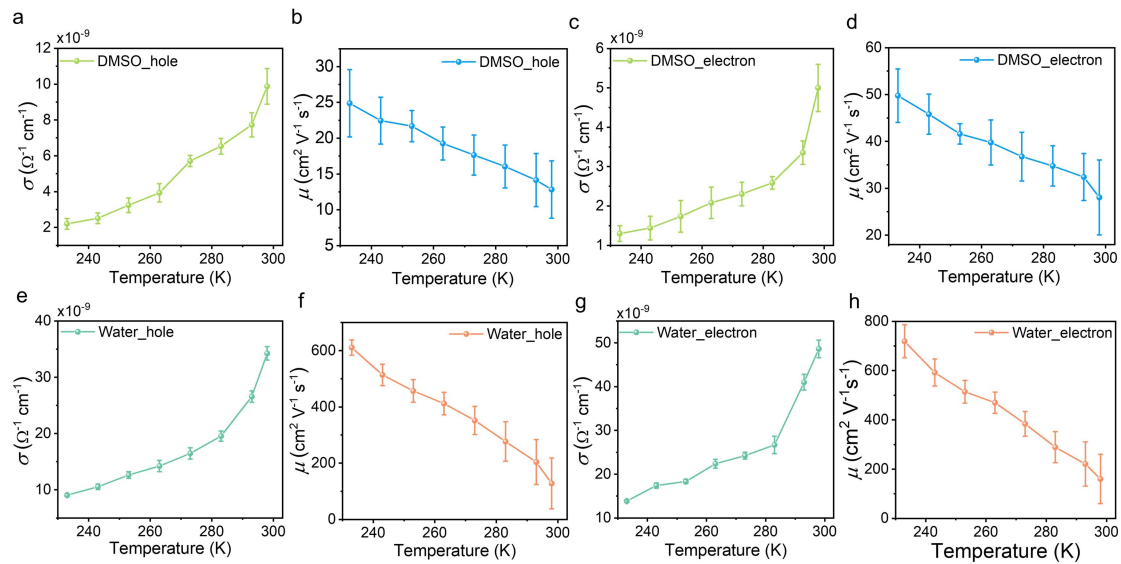
Supplementary Figure 12. Temperature-dependent relative permittivity of the CsPbBr₃ SCs grown in (a) DMSO and (b) water, comparison of the permittivity in dark and under 100 mW cm⁻² white light illumination of the CsPbBr₃ SCs grown in (c) DMSO and (d) water. The insets are the equivalent circuits for extracting of the capacitance values, where C_p is the parallel capacitance, R_p is the parallel resistance and DUT is the device under test.



Supplementary Figure 13. Reproducibility of the J - V curves of (a) hole only devices based on DMSO-grown crystals, (b) electron only devices based on DMSO-grown crystals, (c) hole only devices based on water-grown crystals and (d) electron only devices based on water-grown crystals, obtained from three batches of devices with five continuous scans at room temperature.



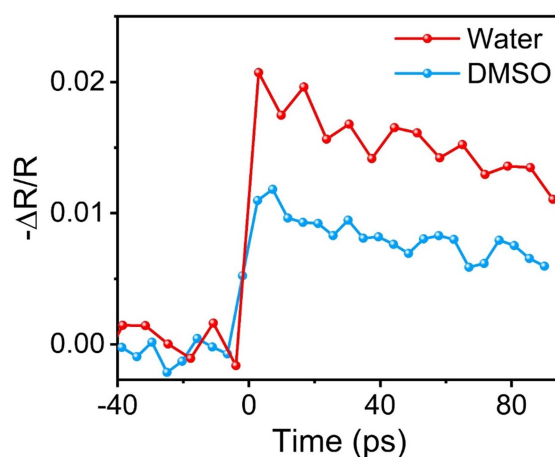
Supplementary Figure 14. (a) Typical scan rate and polarity dependent I-V curves of the CsPbBr₃ based devices and (b) I-V curves collected at the same scan rates for a number of continuous scans.



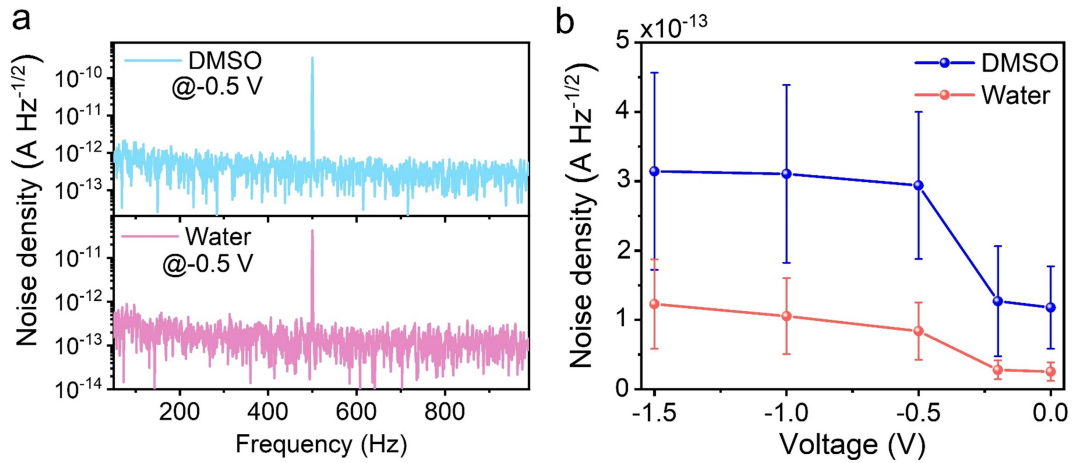
Supplementary Figure 15. Comparison of the calculated electrical properties based on the SCLC method. (a) Conductivity and (b) mobility of the hole-only device based on CsPbBr₃ SCs grown in DMSO, (c) conductivity and (d) mobility of the electron-only device based on CsPbBr₃ SCs grown in DMSO, (e) conductivity and (f) mobility of the hole-only device based on CsPbBr₃ SCs grown in water, (g) conductivity and (h) mobility of the electron-only device based on CsPbBr₃ SCs grown in water.

Supplementary Table 1. Comparison of the calculated electrical properties based on the SCLC measurements.

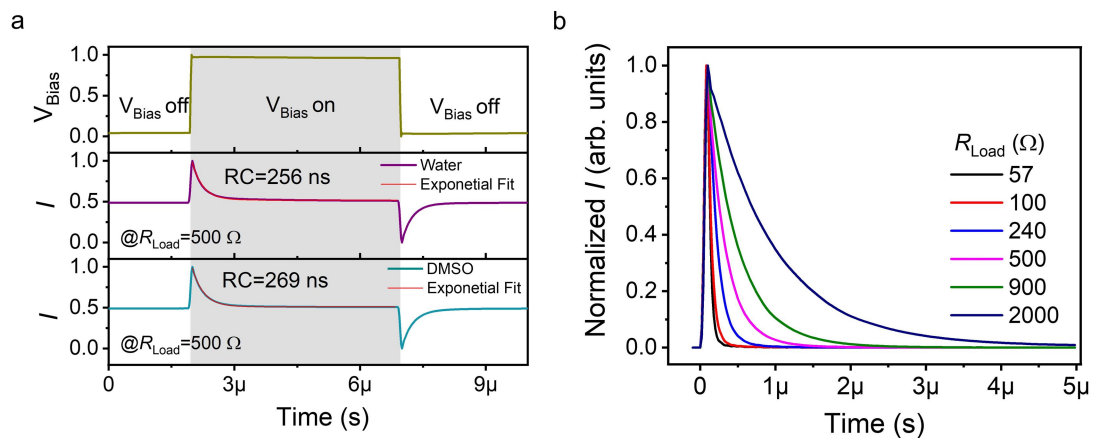
Temperature (K)	Conductivity ($\times 10^{-9} \Omega^{-1} \text{ cm}^{-1}$)	DMSO_hole/electron		Water_hole/electron		
		Trap density ($\times 10^9 \text{ cm}^{-3}$)	Mobility ($\text{cm}^2 \text{ V}^{-1} \text{ s}^{-1}$)	Conductivity ($\times 10^{-9} \Omega^{-1} \text{ cm}^{-1}$)	Trap density ($\times 10^9 \text{ cm}^{-3}$)	Mobility ($\text{cm}^2 \text{ V}^{-1} \text{ s}^{-1}$)
298	9.9/5.0	75.6/71.3	12.8/28.5	34.2/48.6	17.1/22.0	128/160
293	7.7/3.4	64.0/67.5	14.1/32.4	26.6/41.0	13.7/19.6	204/221
283	6.5/2.6	56.9/55.5	16.0/34.8	19.5/26.7	12.1/16.9	277/289
273	5.7/2.3	54.1/50.9	17.7/36.8	16.5/24.2	10.1/15.2	352/384
263	3.9/2.1	52.9/48.9	19.3/39.8	14.2/22.4	8.7/14.2	412/470
253	3.2/1.7	50.9/46.3	21.7/41.6	12.6/18.3	8.0/12.9	457/514
243	2.5/1.4	46.5/42.0	22.5/45.8	10.5/17.4	7.4/11.8	514/592
233	2.2/1.3	41.8/34.1	24.9/49.8	9.0/13.9	6.4/9.8	611/719



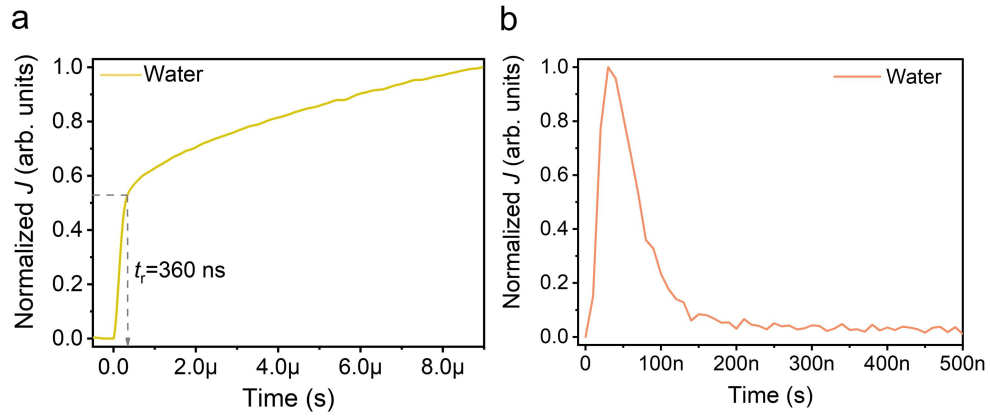
Supplementary Figure 16. Photoconductivity decay of the CsPbBr₃ SCs grown in DMSO and water, obtained via optical-pump-THz-probe spectroscopy (OPTPS) in a reflection geometry at room temperature. The SCs were photoexcited by ultrafast laser pulses at wavelength of 400 nm and fluence of 37 $\mu\text{J cm}^{-2}$.



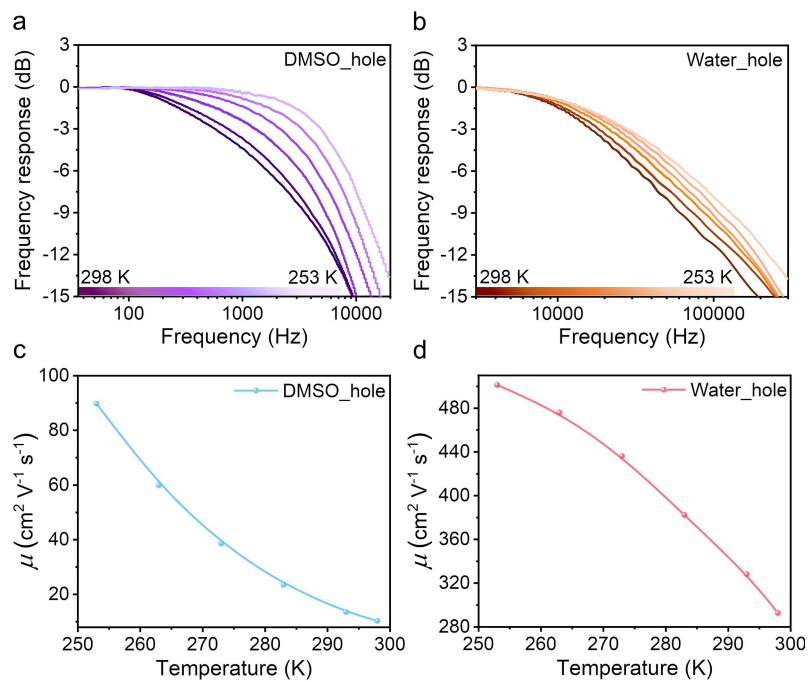
Supplementary Figure 17. (a) Noise spectra of the devices based on CsPbBr₃ SCs grown in DMSO and water under 500 Hz modulated weak light illumination (~ 3 nW cm⁻²), (b) voltage dependent noise current measured at 1 kHz.



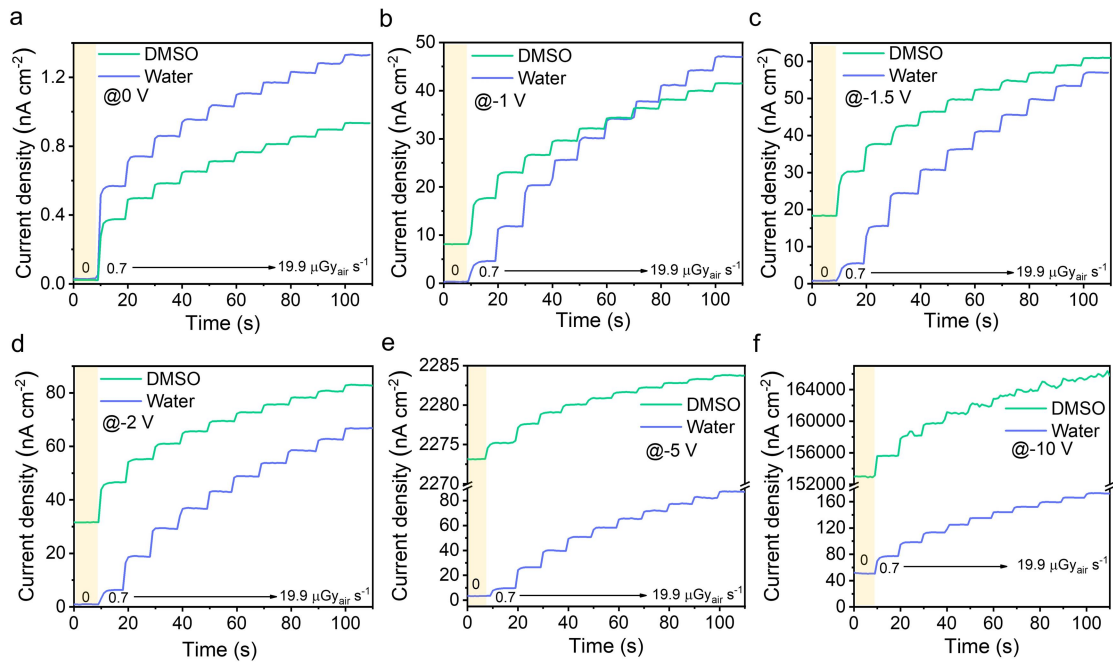
Supplementary Figure 18. (a) Recorded RC decay traces of the devices based on DMSO-grown and water-grown crystals, responding to the square-wave modulated bias voltage applied on these single crystal devices, and (b) load resistance dependent RC decay curves.



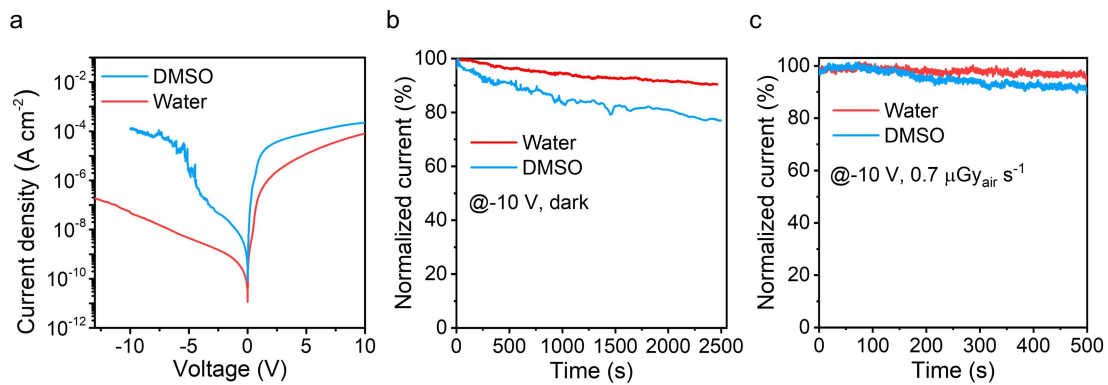
Supplementary Figure 19. The fast photocurrent transient of the detectors based on CsPbBr₃ SCs grown in water (a) under the illumination of a square-wave modulated 528 nm LED, and (b) a 10 ns laser shot.



Supplementary Figure 20. Temperature-dependent frequency response of the devices based CsPbBr₃ SCs grown in (a) DMSO and (b) water, and the inferred carrier mobility of CsPbBr₃ SCs grown in (c) DMSO and (d) water.



Supplementary Figure 21. Comparison of temporal response of the optimized X-ray detectors based on CsPbBr₃ SCs grown in DMSO and water at bias voltages of (a) 0 V, (b) -1 V, (c) -1.5 V, (d) -2 V, (e) -5 V and (f) -10 V, under various X-ray dose rates from 0 to 19.9 μGy_{air} s⁻¹.



Supplementary Figure 22. Comparison of the (a) *J-V* curves measured in the dark with large bias voltage range, bias voltage stability at -10 V (b) in dark and (c) under X-ray illumination with a dose rate of 0.7 μGy_{air} s⁻¹.